

Supporting Information

Selective hydrogenolysis of lignin for sustainable production of 4-propylsyringol over hierarchical CoNC catalysts

Mengqiao Gao,^a Yun Tian,^a Sijie Liu,^{a, b*} Wanying He,^a Xinjun He,^a Kejia Wu,^a Jinxing Long,^a Qiang Zeng,^a and Xuehui Li^{a*}

^a The Guangdong Provincial Laboratory of Green Chemical Technology, School of Chemistry and Chemical Engineering, South China University of Technology, Guangzhou, Guangdong, 510640, China

^b National & Local Joint Engineering Laboratory for Petro-chemicals Materials and Fine Utilization of Resources, Key Laboratory of Chemical Biology and Traditional Chinese Medicine Research (Ministry of Education), College of Chemistry & Chemical Engineering, Hunan Normal University, Changsha, Hunan, 410081, China

CONTENT

Corresponding authors

Sijie Liu, Email: sjliu@hunnu.edu.cn

Xuehui Li, Email: cexhli@scut.edu.cn

1. Experimental section

1.1 Chemicals and materials

1.2 Characterization of catalyst

1.3 Lignin depolymerization and product separation

1.4 Product analysis

1.5 Lignin characterization

1.6 Static adsorption measurements

1.7 Electron paramagnetic resonance measurements

1.8 Determination of the adsorption energy of lignin model compounds

1.9 Catalyst reusability and regeneration

2. Preparation of model compounds

Fig. S1 Treating bagasse lignin with CoNC_{M4} under the optimized condition forms 4-propylsyringol with 8.3 wt.% isolated yields.

Fig. S2 MS spectra of 4-PS.

Fig. S3 ^1H and ^{13}C NMR of 4-propylsyringol.

Fig. S4 TEM of CoNC_{M4} .

Fig. S5 HAADF-STEM images and EDS mappings of (a) CoNC_{M1} , (b) CoNC_{M2} , (c) CoNC_{M3} , (d) Co/NC_{M4} .

Fig. S6 XPS N1s of $\text{CoNC}_{\text{M4-KOH}}$ and $\text{NC}_{\text{M4-KOH}}$.

Fig. S7 (a) The first derivative curves of Co K-edge XANES for Co foli, CoO, CoNC_{M4} and Co_2O_3 , respectively. (b) Fitted valence states of CoNC_{M4} .

Fig. S8 (a) SEM of the reused and regenerated of CoNC_{M4} . (b) N_2 adsorption-desorption

isotherms and (c) comparison of the pore distribution of the fresh, reused and regenerated CoNC_{M4}.

Fig. S9 TG (a) and DSC (b) of lignin, CoNC_{M4}, CoNC_{M4}+lignin and spent CoNC_{M4}.

Fig. S10 XPS of C1s (a), N1s (b) and Co2p (c) of the fresh, reused and regenerated CoNC_{M4}.

Fig. S11 FT-IR spectra of the raw-lignin, Re-lignin-blank and Re-lignin-CoNC_{M4}.

Scheme S1. Control experiments used to determine the reaction pathway.

Table S1 Comparison of reductive catalytic fractionation results over different catalyst in literatures.

Table S2 Pore structure of catalysts.

Table S3 Element analysis of the CoNC catalysts.

Table S4 N atomic relative content ratio and acidity of CoNC.

Table S5 EXAFS fitting parameters at the Co K-edge various samples ($S_0^2=0.71$).

Table S6 Co and N atomic content ratio of CoNC_{M4}.

Table S7 Catalytic of various lignin samples over CoNC_{M4} catalyst.

1. Experimental section

1.1 Chemicals and materials

Sodium lignosulfonate was purchased from TCI. Cobalt acetate, zinc acetate dihydrate, potassium acetate and potassium hydroxide were provided by Tianjin Fuchen chemical reagents factory. DMSO-*d*₆, Pd/C (5% Pd, contains 40-60% H₂O) and Ru/C (5% Ru, contains 50% H₂O) were obtained from Aladdin. Co₃O₄ and 5,5-dimethyl-1-pyrroline N-oxide (DMPO) were purchased from Macklin. benzyloxybenzene (**a1**), dibenzyl ether (**a2**) and benzyloxybenzene (**a3**) were provided by Energy Chemical. 2-phenoxy-1-phenethanol (**a4**), 2-(2-methoxyphenoxy)-1-phenylethanol (**a5**) and 2-(2,6-Dimethoxyphenoxy)-1-phenylethanol (**a6**) were synthesized according to a previously reported method¹ with minor modifications, the synthesis process and structural characterization data are provided in the Supporting Information. The organosolv lignins were separated from the lignocellulosic resources of bagasse, wheat straw, bamboo, corncob, birch, poplar, pine and Chinese fir according to the procedures shown in previous study.²

1.2 Characterization of catalyst

The cobalt contents in the CoNC catalysts were determined by an inductively coupled plasma optical emission spectrometer (ICP-OES) Optima 8300. The C, H, N and S contents of CoNC were determined by Vario EL cube (Germany), and the O content was calculated by conservation of mass based on the assumption that the sample only contains Co, C, H, N, S and O.

Nitrogen adsorption-desorption experiments were conducted on the Micromeritics ASAP 2460 instrument to accurately determine the specific surface area and pore properties of

catalysts. Prior to testing, the catalysts underwent a degassing process at 120°C for 12 h under a pressure of 133 Pa. Subsequently, the samples were subjected to the static-volumetric method at -196°C on the instrument. The specific surface area was determined utilizing the Brunauer-Emmett-Teller (BET) method, while the pore volume was evaluated through the Barrett-Joyner-Halenda (BJH) method.

The crystal phases of catalysts were examined by the powder X-ray diffraction (XRD) patterns (Bruker D8 Advance) with a Cu K α radiation. Raman spectra of the CoNC catalysts were recorded on a LabRAM Aramis (HORIBA) Raman Spectroscopy System. Scanning electron microscopy (SEM) images were obtained on a Hitachi FESEM SU 8220 instrument operating at 5 kV. The transmission electron microscope (TEM) and high-resolution transmission electron microscope (HRTEM) images were obtained on the Rigaku JEOL JEM-2100F TEM operated at 200 kV. The aberration-corrected high-angle annular dark-field scanning transmission electron microscopy (AC-HAADF-STEM) tests were performed using JEM-200F (JEOL, Tokyo, Japan). X-ray photoelectron spectroscopy (XPS) was performed on an AXIS SUPRA+ (Kratos) instrument with a monochromate Al K α anode. All binding energy calculations were calibrated using the peak position of C1s at 284.8 eV. The X-ray absorption near edge structure (XANES) and extended X-ray absorption fine structure (EXAFS) data were acquired at RapidXAFS HE Ultra, and energy calibration using Co foil. The raw data were background deducted and Fourier transformed using Athena software, and the data fitted was performed using Demeter software.

NH₃ temperature programmed desorption (NH₃-TPD) patterns were recorded by a BELCAT II instrument with a thermal conductivity detector (TCD) and a quadrupole mass

spectrometer. In a typical experiment, 100 mg sample was heated at 120°C for 5 h to remove the physisorbed species like water and CO₂. Then the sample was cooled to 50°C in a He stream, and further flushed with a flow of 5% (v/v) NH₃ diluted with He (total flow rate of 20 mL min⁻¹) for 1 h. Afterwards, the sample was flushed with flowing He (20 mL min⁻¹) for another 1 h to ensure complete removal of physisorbed species. Then, the samples were heated to 900°C in the He stream at a rate of 10°C min⁻¹ and the amount of NH₃ desorbed was monitored by a TCD. The mass spectrometer followed the NH₃ desorption by $m/z = 17$.

Thermogravimetric analysis (TGA) and differential scanning calorimetry (DSC) were performed on a NETZSCH STA 449 F5 instrument. Approximately 5-10 mg of sample was heated from room temperature to 900°C at a rate of 10°C/min in air flow (50 mL/min). The mixtures (CoNC_{M4}+Lignin) were prepared by static adsorption experiment method, which will be introduced in the following section.

1.3 Lignin depolymerization and product separation

100 mg organosolv lignin, certain amounts of catalyst and 10 mL ethanol were put into a 50 mL stainless autoclave (Labe Scientific Instrument Co., Ltd., Shanghai, China). The air inside the autoclave was replaced with pure hydrogen three times. Then, the autoclave was pressurized to 1.0 MPa using hydrogen and heated to a desired temperature (190-270°C) with a heating rate of 10°C min⁻¹. After maintaining at the final temperature for a designated time (2-6 h), the autoclave was rapidly cooled to room temperature and the mixture in reactor was separated by using filtration. The solid fraction, which mainly contained catalyst, was washed with THF three times (4 mL × 3). Subsequently, the resulting solid fraction was dried at 120°C until no significant weight loss, then it was employed in the next run for investigating its reusability.

The THF wash solution was combined with the filtrate above and diluted to 25 mL for further analysis. 2 mL of the above diluted solution was used for quantitative and qualitative analysis. 200 mL deionized water was then added into the left diluted solution, yielding a flocculent precipitate. This flocculent precipitate composing unconverted or partly-converted lignin, was separated using filtration, so obtained solid was then dried at 80°C under a reduced pressure until constant weight. The recovered lignin was finally obtained and designated as Re-lignin.

1.4 Product analysis

The analysis of monophenols was conducted on a GC-MS-FID instrument (Agilent 7890B/5977A). The NIST Mass Spectral Search Program was employed to conduct qualitatively identification. An FBX-5MS PLUS gas chromatography column (30 m×0.25 μm×0.25 mm) was used for product separation with 1.0 mL min⁻¹ He as the carrier gas. The temperature of injector and detector was set at 280°C. The oven temperature started at 50°C (held for 1 min), then ramped to 250°C at a rate of 10°C min⁻¹ and held for 6 min. Dimethyl phthalate was used as internal standard for quantitatively analysis. Each experimental was repeated three times and the results were averaged. The conversion of lignin was calculated based on the weight comparison of regenerated lignin (Re-lignin) and raw lignin (eqn.1), the yield of products was determined based on the quality of the volatile products and the raw lignin (eqn.2). The selectivity of 4-PS was calculated through the weight percentage of 4-PS in the total volatile products (eqn.3).

$$\text{Conversion(\%)} = \frac{W_O - W_R}{W_O} \times 100\% \quad (1)$$

$$\text{Yield(wt.\%)} = \frac{W_{VP}}{W_O} \times 100\% \quad (2)$$

$$\text{Selectivity}(\%) = \frac{W_{4-PS}}{W_{VP}} \times 100\% \quad (3)$$

Where W_O , W_R , W_{4-PS} and W_{VP} were the weights of organosolv lignin, Re-lignin, 4-PS and the volatile products, respectively.

1.5 Lignin characterization

The molecular weight distributions of raw lignin and Re-lignin samples were obtained by a gel permeation chromatography (GPC) using 1.0 mL min^{-1} tetrahydrofuran (THF) as the eluent, the oven temperature was set at 35°C . The two-dimensional heteronuclear single quantum correlation nuclear magnetic resonance (2D HSQC NMR) of raw lignin and Re-lignin were recorded on a Bruker NMR spectrometer (Avance III 600 MHz), 80 mg of sample was dissolved in 0.6 mL of DMSO-*d*₆ (D.99.8%, TMS 0.03%), the spectrometer frequency was 500.19/125.77 Hz, and the spectral width was 5882.4/20752.3 Hz for $^1\text{H}/^{13}\text{C}$ and the relaxation delay was set at 1.5 s. The ^1H -NMR and ^{13}C -NMR of samples were recorded on a Bruker NMR spectrometer (Avance III 600 MHz) as well. Fourier transform infrared (FT-IR) analysis of raw lignin and Re-lignin were performed using a Thermo Scientific Nicolet iS10 instrument. All FT-IR spectra were scanned 64 times at a resolution of 4 cm^{-1} .

1.6 Static adsorption measurements

The static adsorption experiments were carried out to investigate the diffusion behaviour and absorption properties of lignin over different catalysts according to our previous work³. In a typical run, 30 mg lignin and 30 mg catalyst were thoroughly immersed in 30 mL THF, after continuous stirring at room temperature for 24 h, the solid fraction was separated by filtration and washed using fresh THF (20 mL×3). The liquid fraction was combined with that used for solid washing, and then it was concentrated under reduced pressure to remove THF. The

unabsorbed lignin was then obtained as a brown solid. Subsequently, this unabsorbed lignin and a certain amount of internal standard (dimethyl terephthalate) were dissolved into 0.5 mL DMSO-*d*₆. The adsorption capacities of different CoNC catalysts for lignin were measured by the areas of ¹H NMR at the chemical shift of 10.01 ppm of lignin (phenolic protons)⁴ and 8.14 ppm of dimethyl terephthalate (aromatic protons).⁵

1.7 Electron paramagnetic resonance measurements

The electron paramagnetic resonance (EPR) was recorded at 20°C and maintained its operating temperature by circulating water. Spectral scanned with a center field of 3505 G, sweep width of 100 G, modulation amplitude of 2 G, receiver gain of 10 dB. Samples for EPR testing were reacted with water solvent under optimal conditions (230°C, 1 MPa H₂). 1 mL of reaction solution was collected by real-time sampling and quickly cooled to room temperature in an ice water bath. Subsequently, 0.01 g DMPO was dissolved into the above sample. The resulting mixture was subjected to EPR testing.

1.8 Determination of the adsorption energy of lignin model compounds

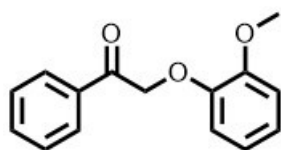
Adsorption energy calculations were performed using three model compounds, 2-phenoxy-1-phenethanol (**a4**), 2-(2-methoxyphenoxy)-1-phenylethanol (**a5**) and 2-(2,6-Dimethoxyphenoxy)-1-phenylethanol (**a6**), representing the H, G and S units of the lignin structure, respectively. All geometry optimizations were employed using DMol3 program from the DFT calculation via software Materials Studio. The Effective Core Potentials (ECP)⁶ were treated in the calculations for Co atom, whereas H, C and O were performed as in the all-electron. The generalized gradient approximation (GGA) with a Perdew-Burke-Ernzerh (PBE) of method as the exchange-correlation functional was achieved.⁷ The double numerical plus

polarization (DNP) as the basis set was used. The following convergence standard of total energy was 10^{-5} Ha, the force was 0.002 Ha/Å, and the maximum displacement tolerance was 0.005 Å.

1.9 Catalyst reusability and regeneration

The catalyst after the fourth recycle was regenerated by a water steam activation method. The spent catalyst was heated to 700°C at a speed of $2^{\circ}\text{C min}^{-1}$ in a tube furnace under a flowing N_2 . After holding at the terminal temperature for 30 min, the tube furnace was rapidly heated to 820°C within 12 min. Then, the atmosphere was switched to steam and maintained for 10 min. The regenerated catalyst was thus obtained when the sample cooled down to room temperature under the protection of N_2 .

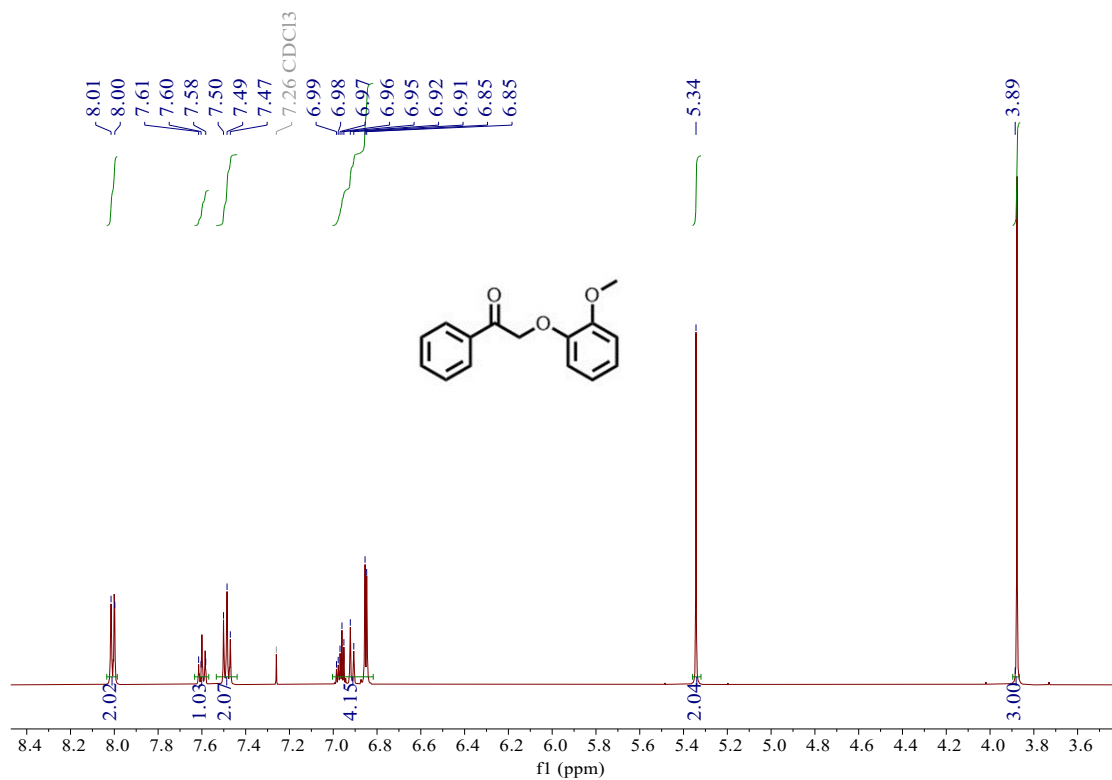
2. Preparation of model compounds

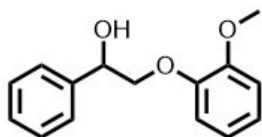
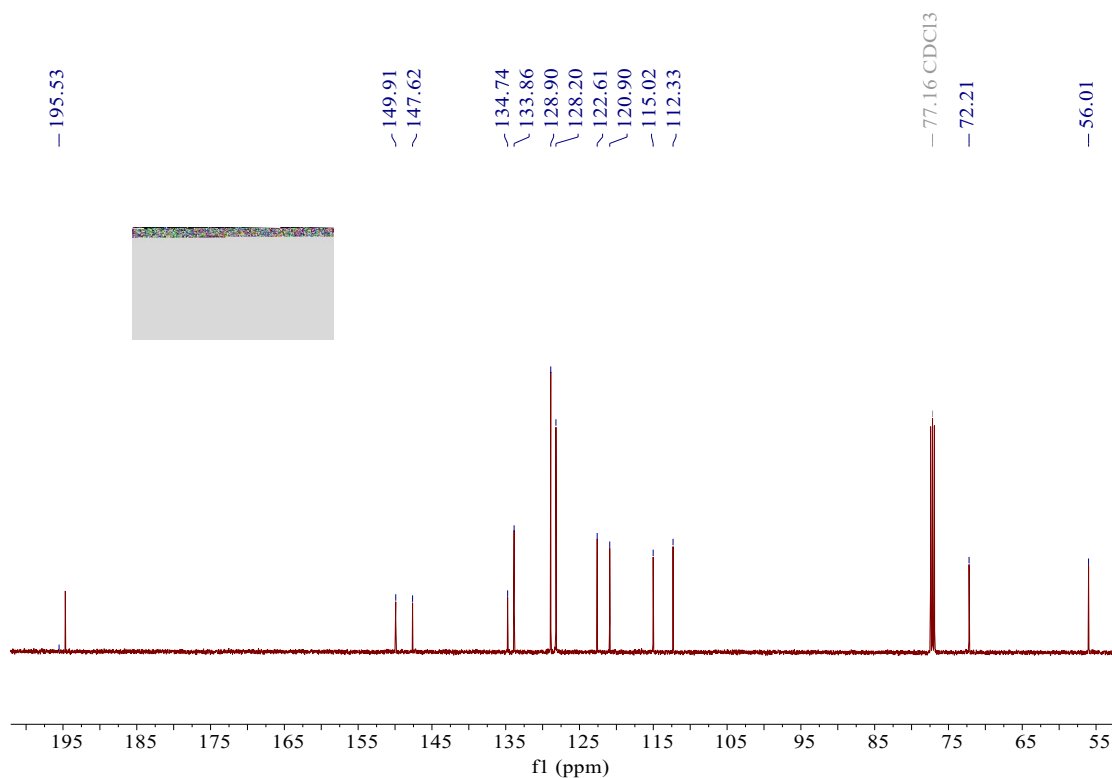


2-(2-Methoxyphenoxy) acetophenone

The 2-bromoacetophenone (10 mmol, 2.0 g) was dissolved in acetone (60 mL) and guaiacol (12 mmol, 1.5 g) was added at RT under vigorous stirring until completely dissolved. K_2CO_3 (70 mmol, 9.67 g) was added to the above solution and refluxed at 60°C . The reaction progression was monitored by thin-layer chromatography (TLC). After the end of the reaction, it was cooled to room temperature, and the organic phase was combined after filtration, and dried over MgSO_4 . The crude product was obtained by concentrating on a rotary evaporator under reduced pressure. 2-(2-Methoxyphenoxy) acetophenone would be obtained by column chromatography (petroleum ether/ethyl acetate 4/1) purification and characterized by NMR spectroscopy. ^1H NMR (500 MHz, CDCl_3) δ 8.01, 8.00, 7.61, 7.60, 7.58, 7.50, 7.49, 7.47, 6.99,

6.98, 6.97, 6.96, 6.95, 6.92, 6.91, 6.85, 6.85, 5.34, 3.89. ^{13}C NMR (126 MHz, CDCl_3) δ 195.53, 149.91, 147.62, 134.74, 133.86, 128.90, 128.20, 122.61, 120.90, 115.02, 112.33, 72.21, 56.01.



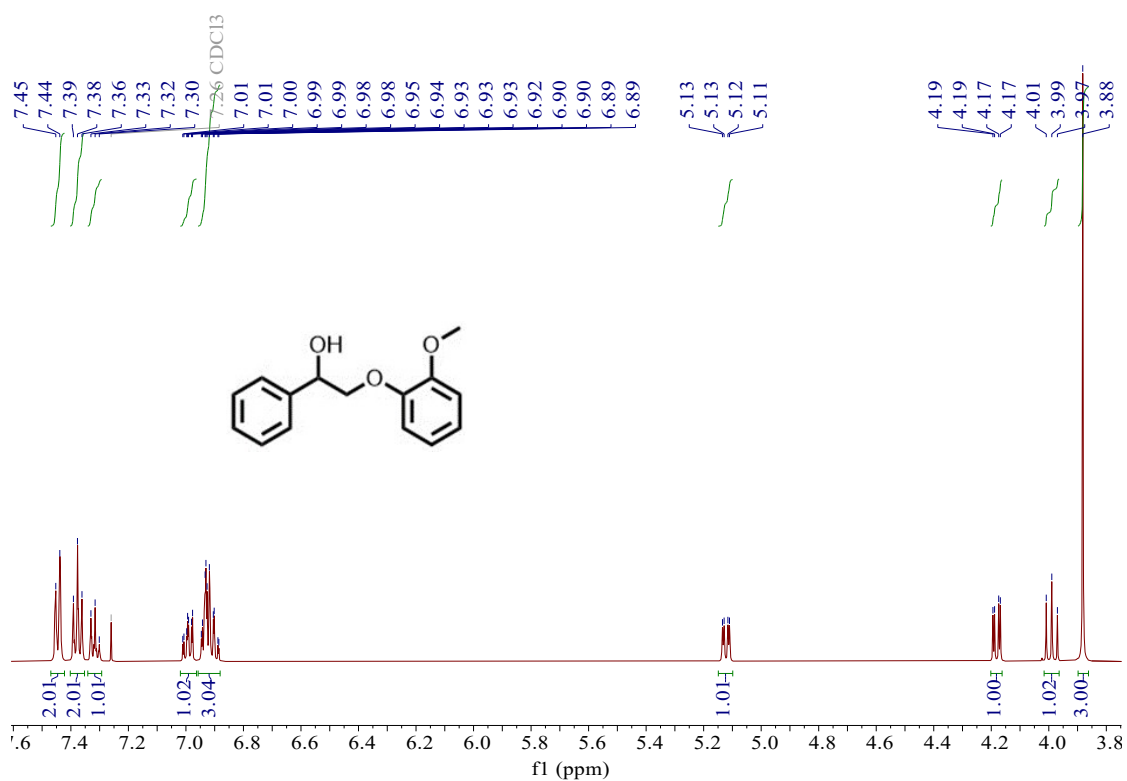


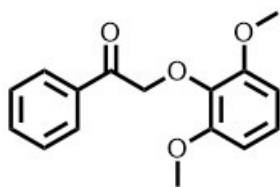
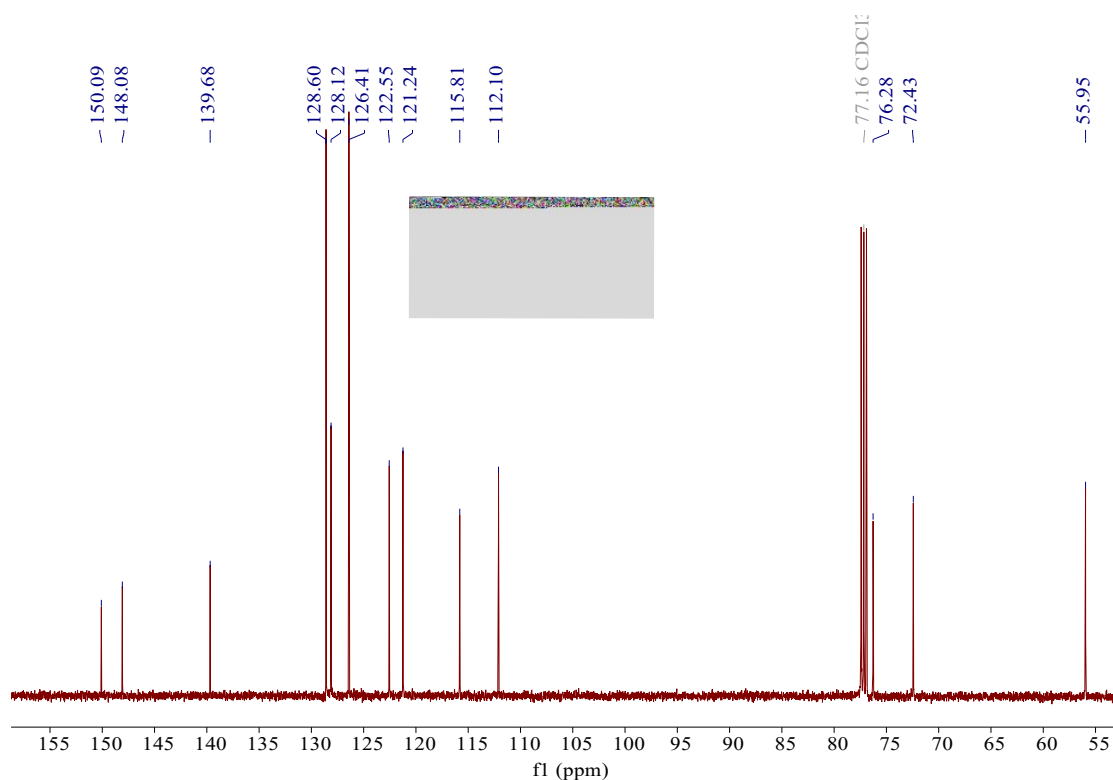
2-(2-Methoxyphenoxy)-1-phenylethanol

The 2-(2-Methoxyphenoxy) acetophenone (8 mmol, 1.9 g) was dissolved in THF (100 mL). An aqueous solution containing NaBH₄ (16 mmol, 0.6 g) was slowly added to the THF solution described above in an ice water bath. The mixture was subjected to continuous stirring in the ice water bath for a duration of 50 minutes, followed by subsequent transfer to ambient room temperature conditions for 4 h. A saturated aqueous solution of NH₄Cl (100 mL) was used for the quenching of the reaction. The organic phase was extracted with EtOAc (3x20 mL), and dried over MgSO₄. Model 1b was obtained by column chromatography (petroleum ether/ethyl

acetate 4/1) purification and characterized by NMR spectroscopy. ^1H NMR (500 MHz, CDCl_3)

δ 7.45, 7.44, 7.39, 7.38, 7.36, 7.33, 7.32, 7.30, 7.01, 7.01, 7.00, 6.99, 6.99, 6.98, 6.98, 6.95, 6.94, 6.93, 6.93, 6.93, 6.92, 6.90, 6.90, 6.89, 6.89, 5.13, 5.13, 5.12, 5.11, 4.19, 4.19, 4.17, 4.17, 4.01, 3.99, 3.97, 3.88. ^{13}C NMR (126 MHz, CDCl_3) δ 150.09, 148.08, 139.68, 128.60, 128.12, 126.41, 122.55, 121.24, 115.81, 112.10, 76.28, 72.43, 55.95.

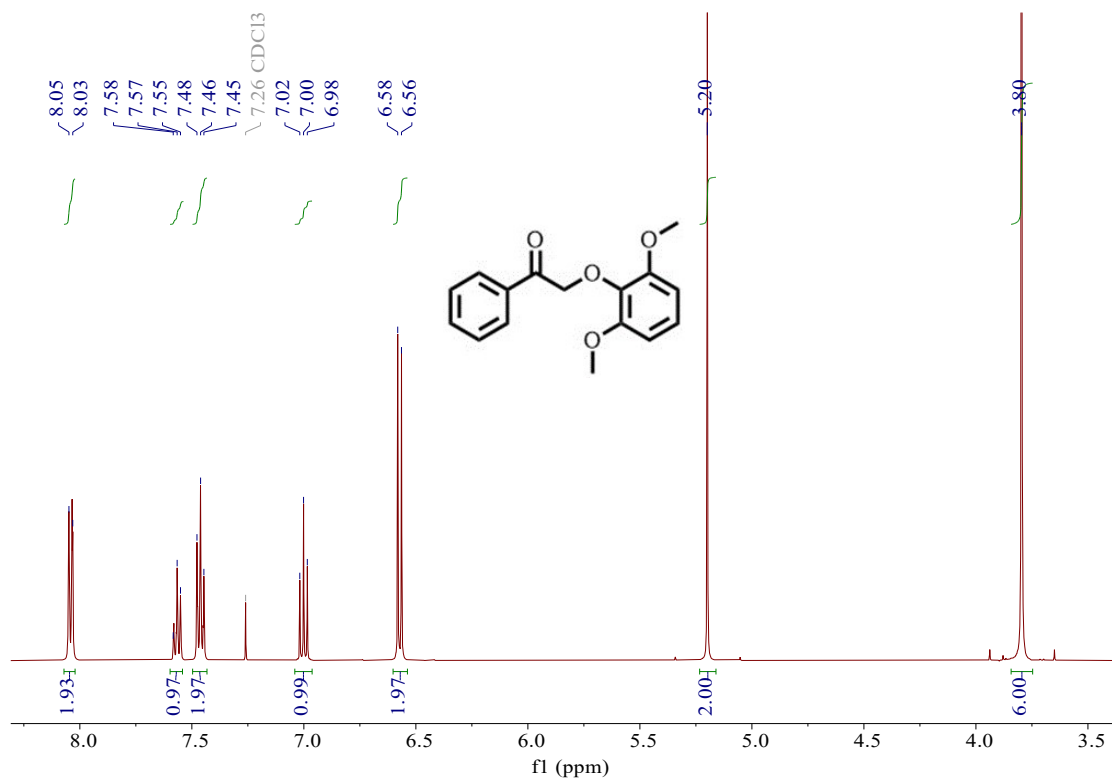


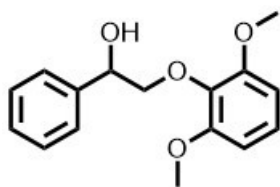
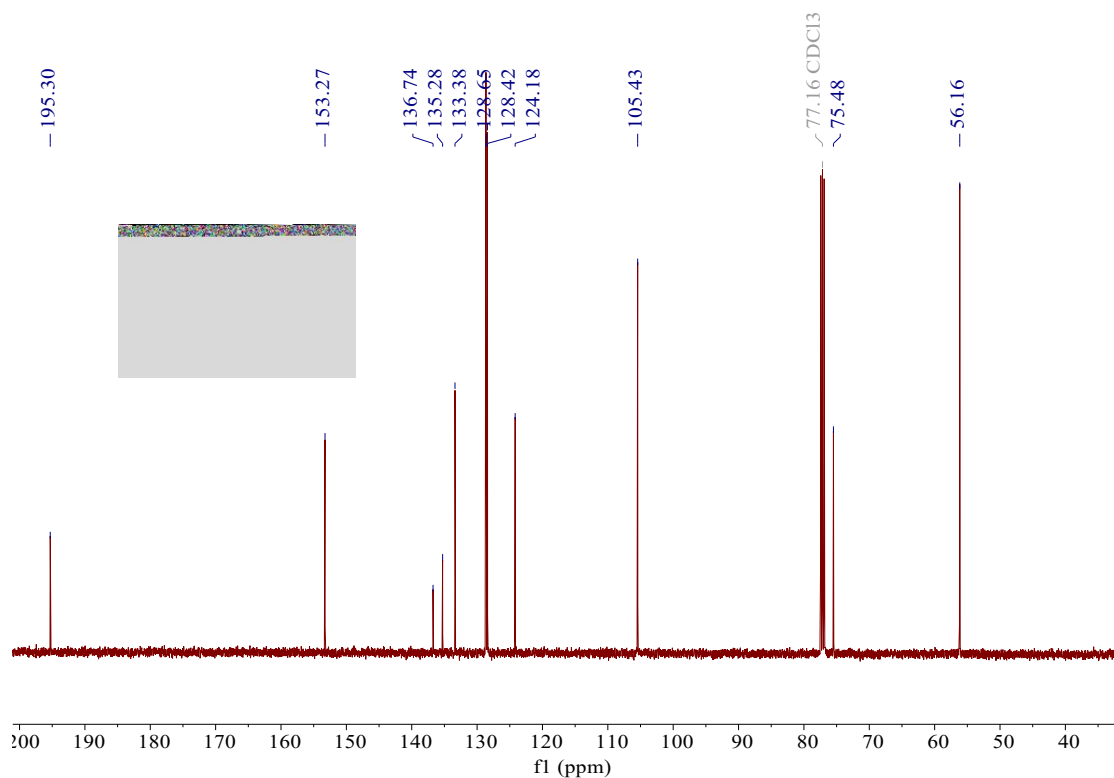


2-(2,6-Dimethoxyphenoxy)-1-phenylethan-1-one

The synthesis method was similar to Model 1b. The 2-bromoacetophenone (10 mmol, 2.0 g) was dissolved in acetone (60 mL) and Syringol (12 mmol, 1.85 g) was added at RT under vigorous stirring until completely dissolved. K₂CO₃ (70 mmol, 9.67 g) was added to the above solution and refluxed at 60°C. The reaction progression was monitored by thin-layer chromatography (TLC). After the end of the reaction, it was cooled to room temperature, and the organic phase was combined after filtration, and dried over MgSO₄. The crude product was obtained by concentrating on a rotary evaporator under reduced pressure. 2-(2,6-Dimethoxyphenoxy)-1-phenylethan-1-one would be obtained by column chromatography

(petroleum ether/ethyl acetate 4/1) purification and characterized by NMR spectroscopy. ^1H NMR (500 MHz, CDCl_3) δ 8.05, 8.03, 7.58, 7.57, 7.55, 7.48, 7.46, 7.45, 7.02, 7.00, 6.98, 6.58, 6.56, 5.20, 3.80. ^{13}C NMR (126 MHz, CDCl_3) δ 195.30, 153.27, 136.74, 135.28, 133.38, 128.65, 128.42, 124.18, 105.43, 75.48, 56.16.

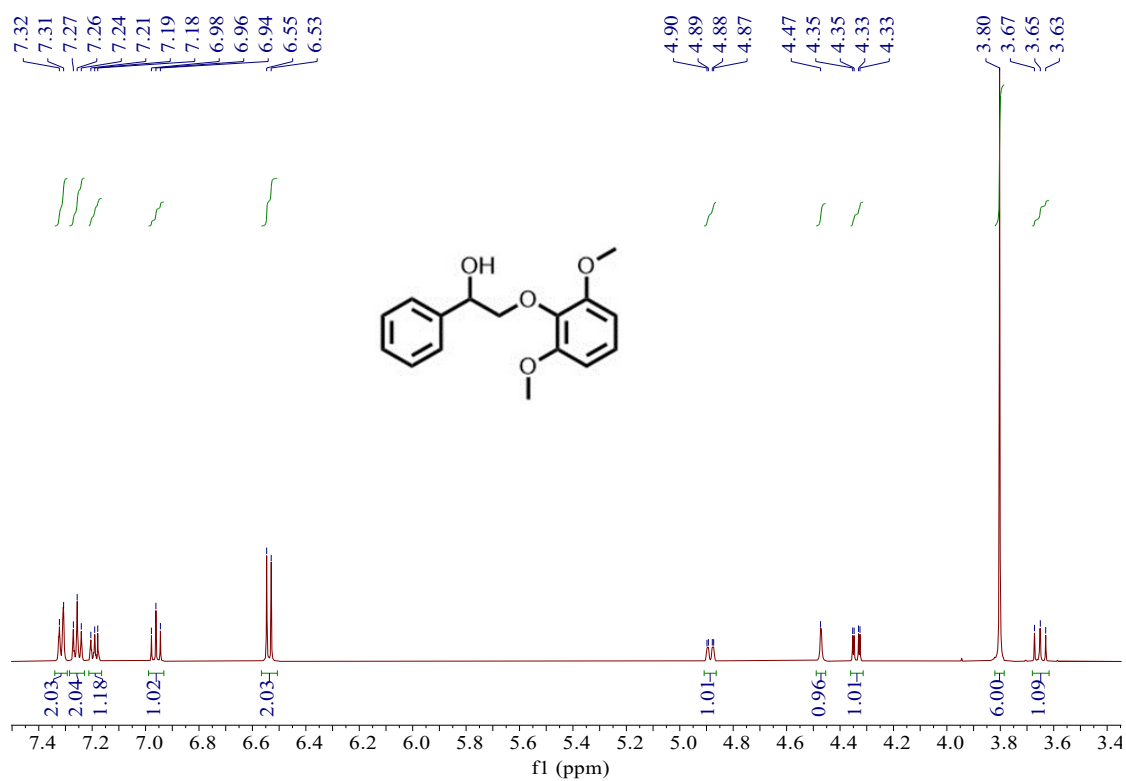


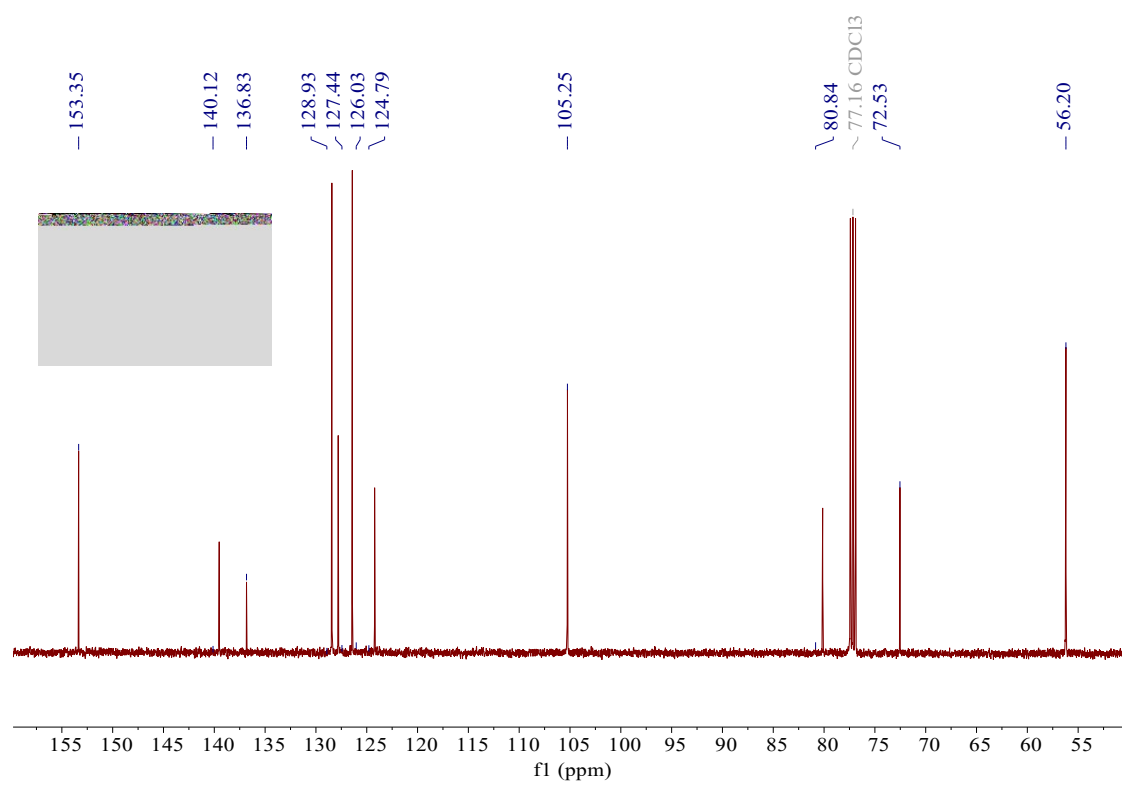


2-(2,6-Dimethoxyphenoxy)-1-phenylethanol

The synthesis method was similar to Model 2b. 2-(2,6-Dimethoxyphenoxy)-1-phenylethanol (8 mmol, 2.2 g) was dissolved in THF (100 mL). An aqueous solution containing NaBH₄ (16 mmol, 0.6 g) was slowly added to the THF solution described above in an ice water bath. The mixture was subjected to continuous stirring in the ice water bath for a duration of 50 minutes, followed by subsequent transfer to ambient room temperature conditions for a period of 4 h. A saturated aqueous solution of NH₄Cl (100 mL) was used for the quenching of the reaction. The organic phase was extracted with EtOAc (3x20 mL), and dried over MgSO₄. Model 2b was obtained by column chromatography (petroleum ether/ethyl acetate 4/1)

purification and characterized by NMR spectroscopy. ^1H NMR (500 MHz, CDCl_3) δ 7.32, 7.31, 7.27, 7.26, 7.24, 7.21, 7.19, 7.18, 6.98, 6.96, 6.94, 6.55, 6.53, 4.90, 4.89, 4.88, 4.87, 4.47, 4.35, 4.35, 4.33, 4.33, 3.80, 3.67, 3.65, 3.63. ^{13}C NMR (126 MHz, CDCl_3) δ 153.35, 140.12, 136.83, 128.93, 127.44, 126.03, 124.79, 105.25, 80.84, 72.53, 56.20.





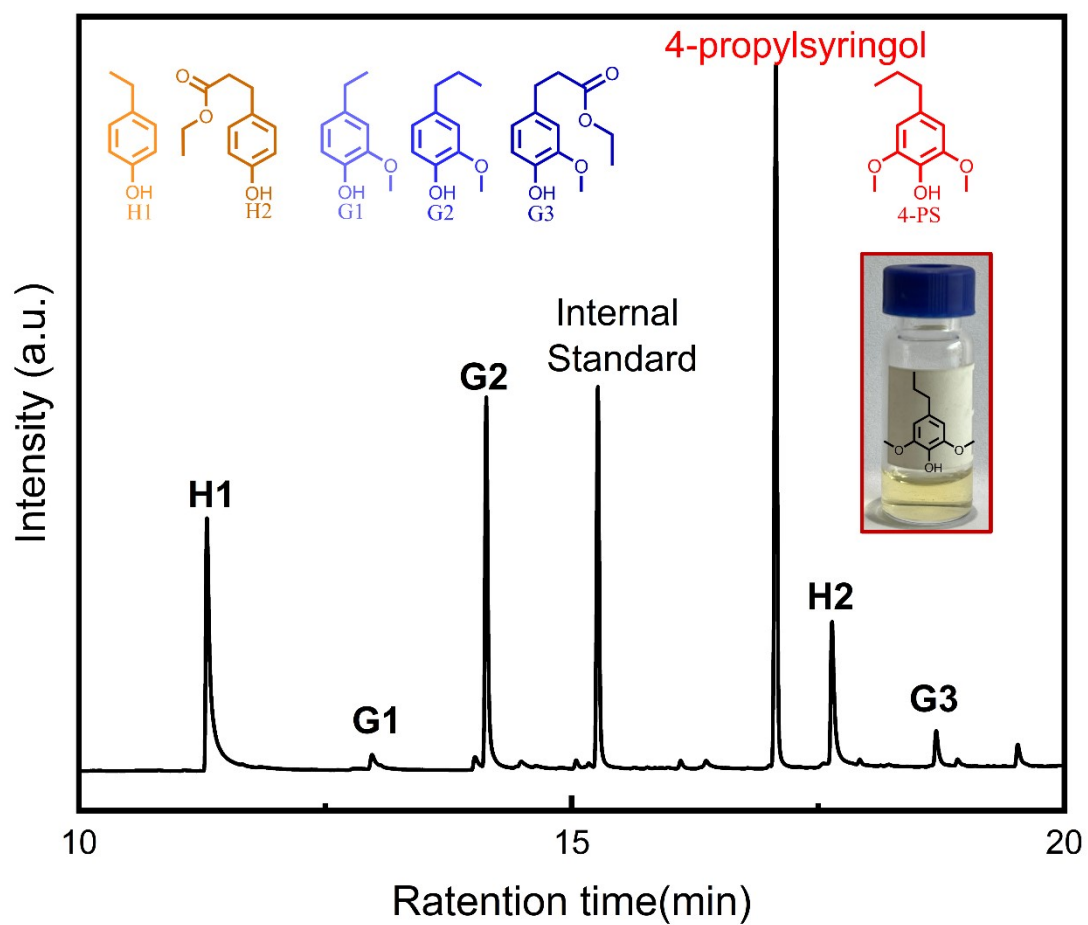


Fig. S1 Treating bagasse lignin with CoNC_{M4} under the optimized condition forms 4-propylsyringol with 8.3 wt.% isolated yields.

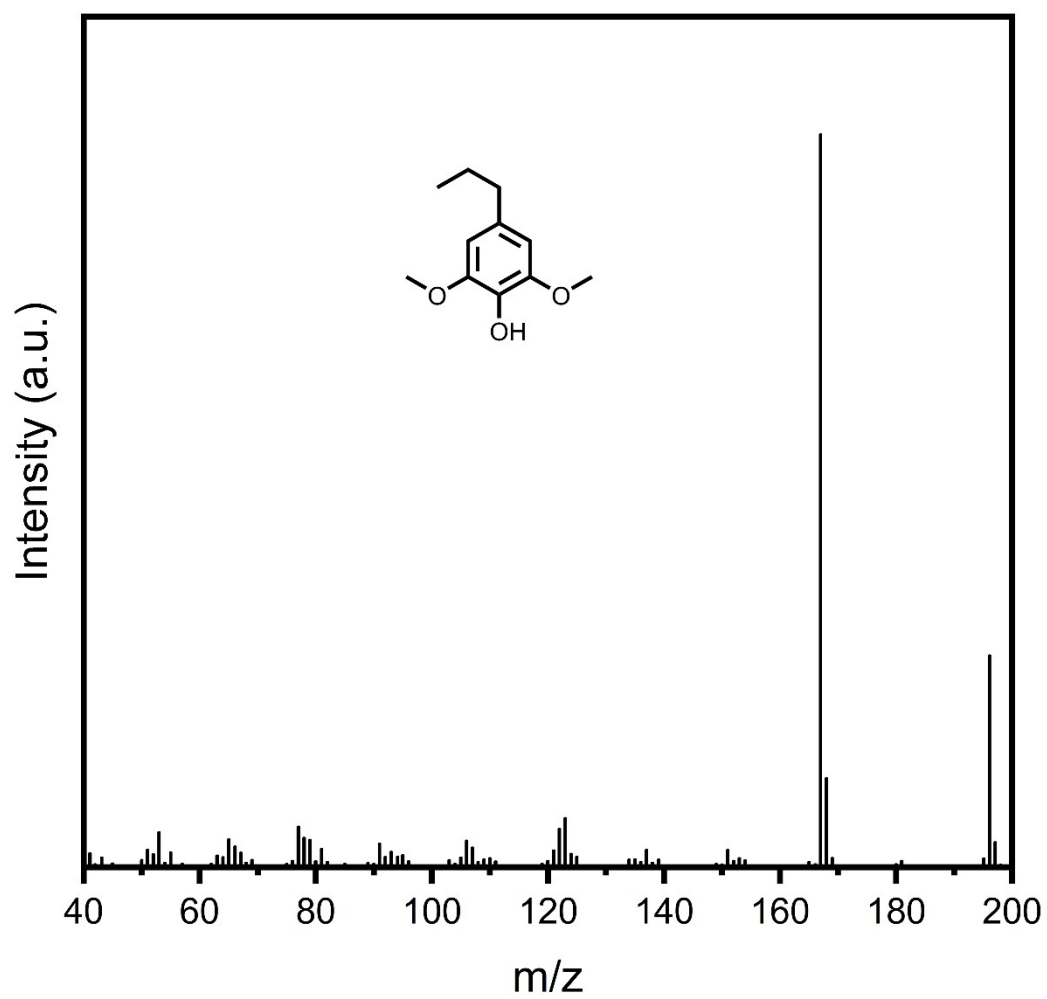
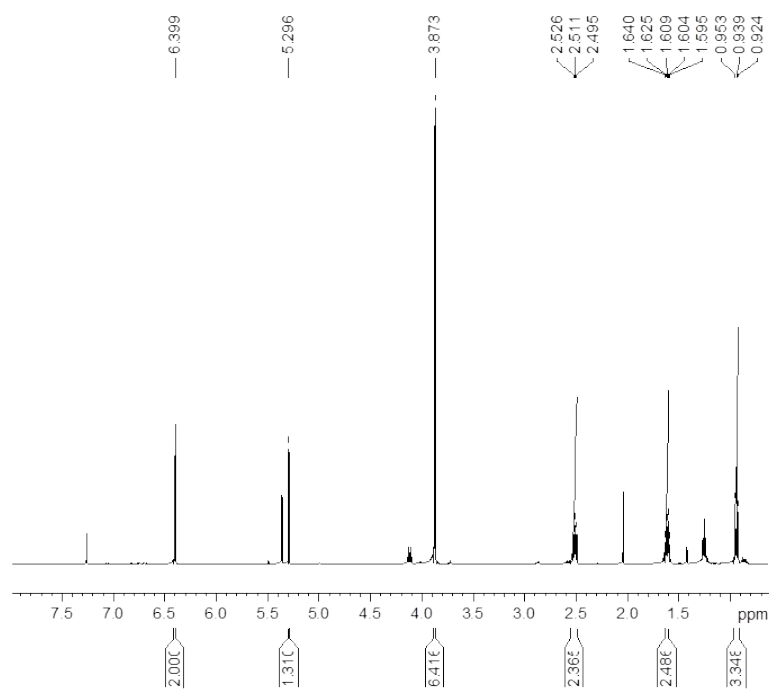
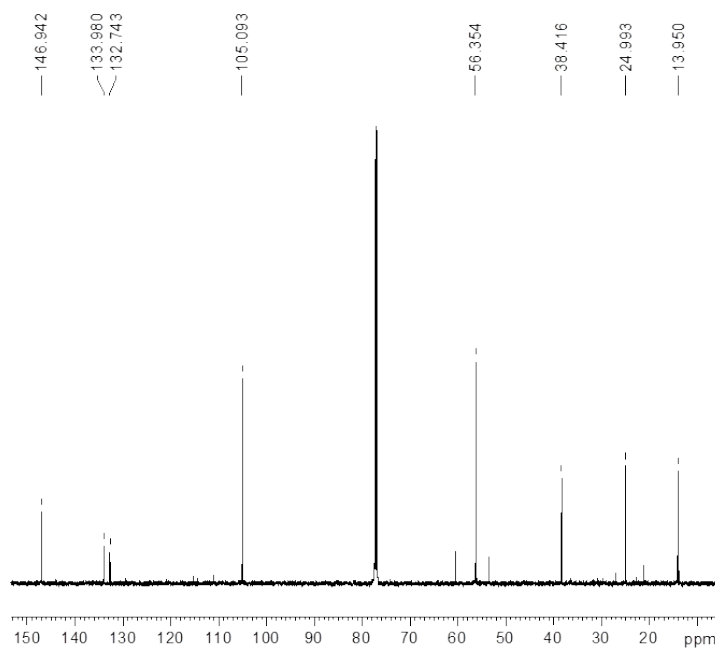


Fig. S2 MS spectra of 4-PS.



^1H NMR (CDCl_3 , 500 MHz) δ (ppm): 6.39(s, 2H, Ar-*H*), 5.30 (s, 1H, Ar-*OH*), 3.87 (s, 6H, Ar-O- CH_3), 2.50-2.53 (t, 2H, Ar- CH_2 - CH_2 -), 1.60-1.64 (m, 2H, - CH_2 - CH_2 - CH_3), 0.92-0.95 (t, 3H, - CH_2 - CH_3).



^{13}C NMR (CDCl_3 , 126 MHz) δ (ppm): 13.95 (- CH_3), 24.99 (- CH_2 -), 38.42 (Ar- CH_2 -), 56.35 (Ar-O- CH_3), 105.9, 132.74, 133.98, 146.94 (ArC).

Fig. S3 ^1H and ^{13}C NMR of 4-propylsyringol.

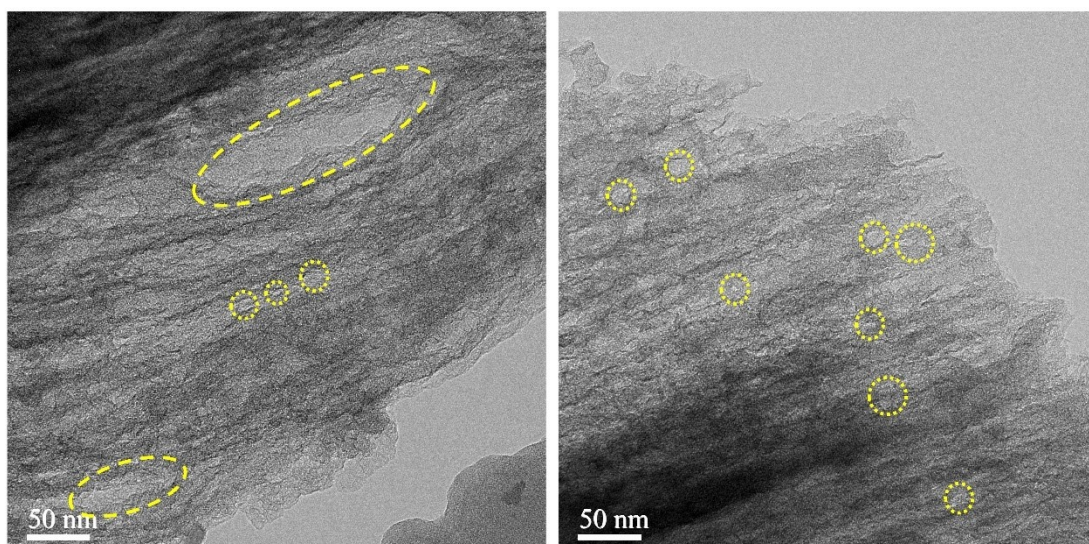


Fig. S4 TEM of CoNC_{M4}.

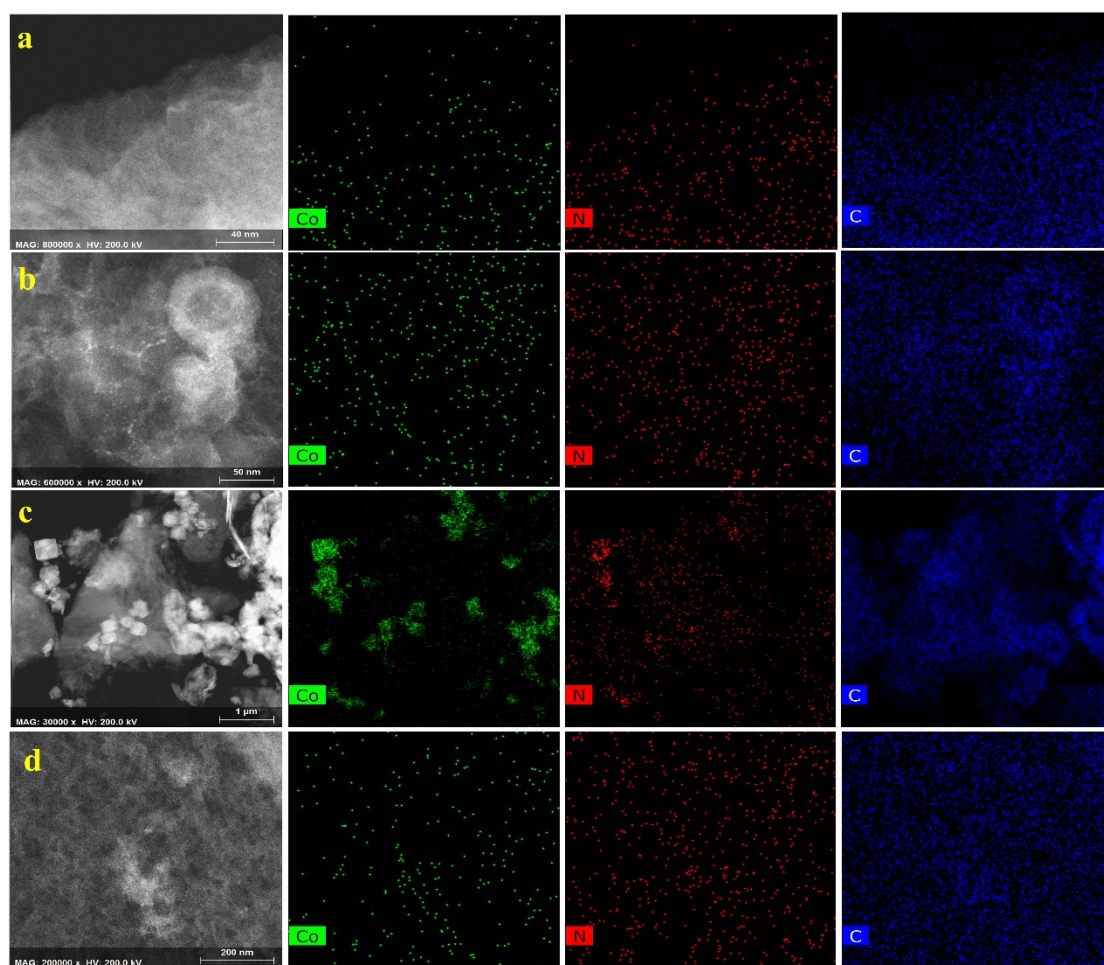


Fig. S5 HAADF-STEM images and EDS mappings of (a) CoNC_{M1}, (b) CoNC_{M2}, (c) CoNC_{M3},

(d) Co/NC_{M4}.

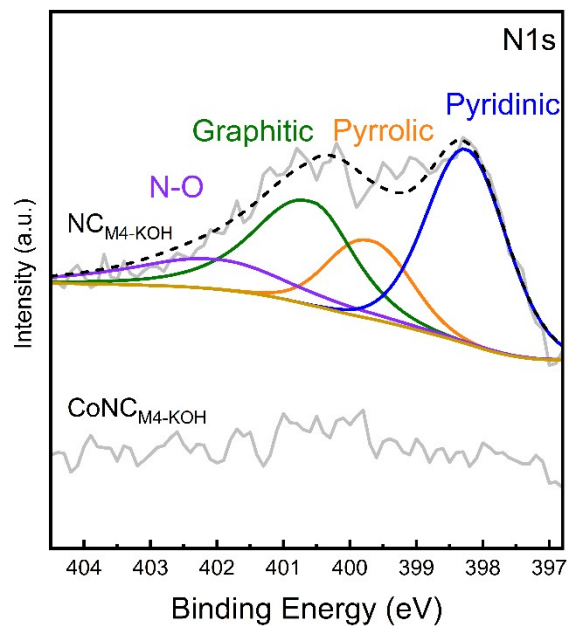


Fig. S6 XPS N1s of CoNC_{M4}-KOH and NC_{M4}-KOH. CoNC_{M4}-KOH and NC_{M4}-KOH: After stirring in a 1 mol L⁻¹ KOH solution for 5 h, the catalyst is filtered to obtain a solid, which is then washed three times with deionized water to obtain the catalyst.

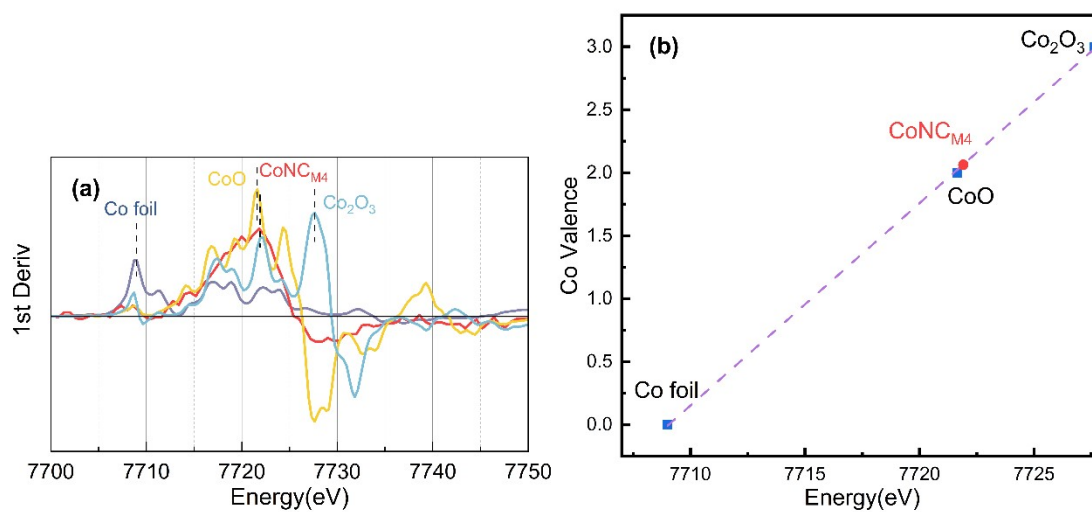


Fig. S7 (a) The first derivative curves of Co K-edge XANES for Co foil, CoO, CoNC_{M4} and Co₂O₃, respectively. (b) Fitted valence states of CoNC_{M4}.

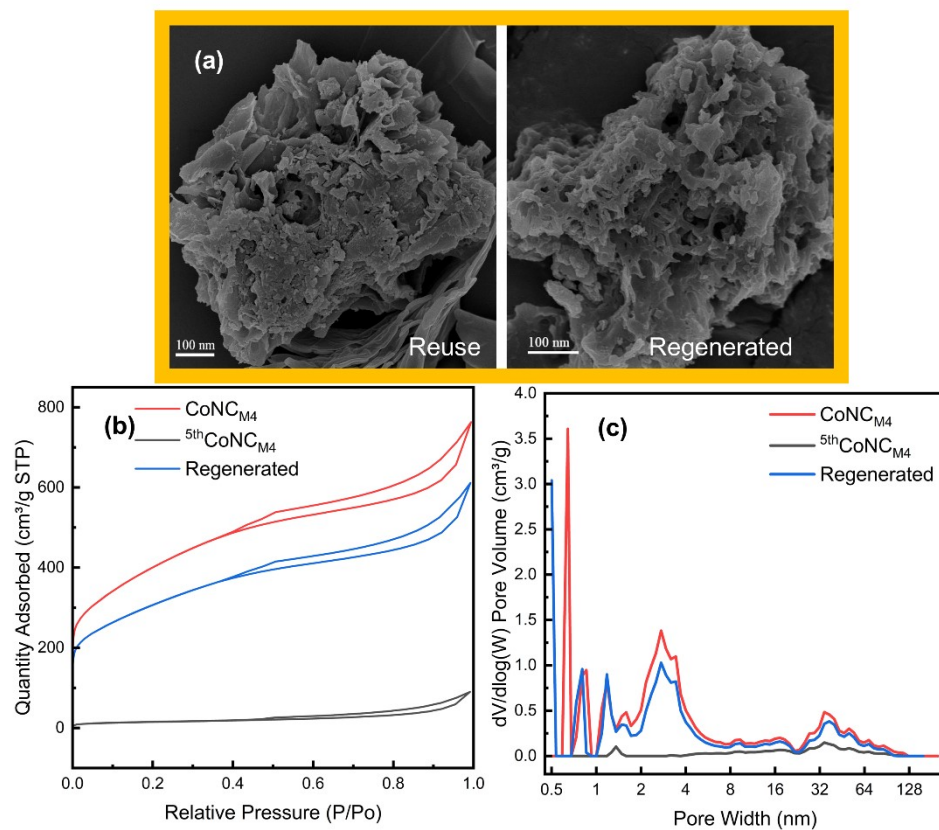


Fig. S8 (a) SEM of the reused and regenerated of CoNC_{M4}. (b) N₂ adsorption-desorption isotherms and (c) comparison of the pore distribution of the fresh, reused and regenerated CoNC_{M4}.

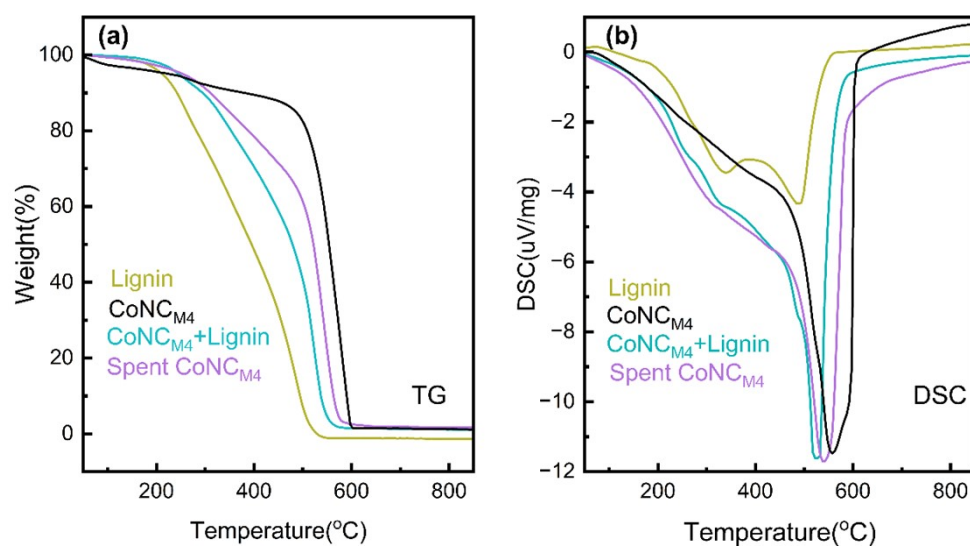


Fig. S9 TG (a) and DSC (b) of lignin, CoNC_{M4}, CoNC_{M4}+lignin and spent CoNC_{M4}.

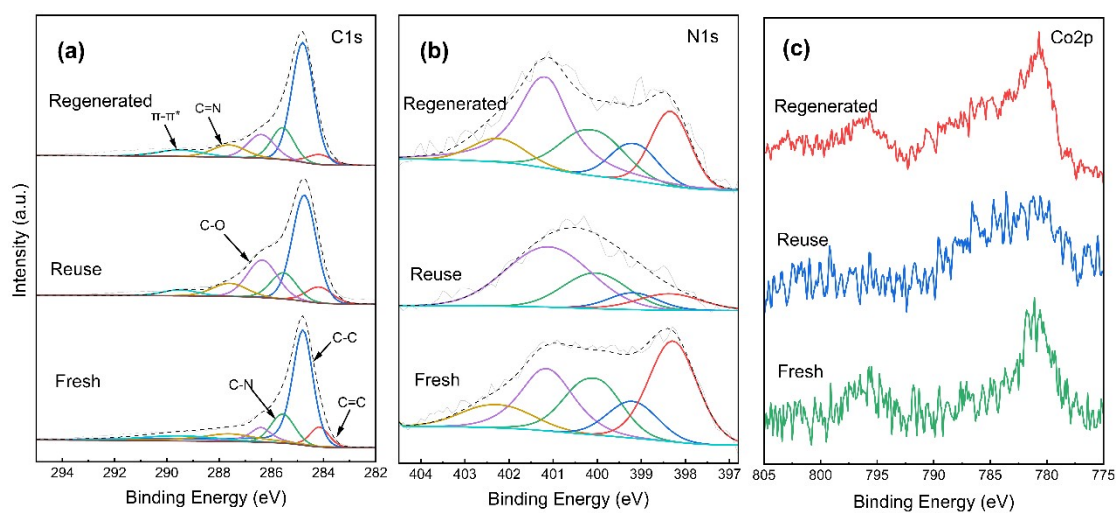


Fig. S10 XPS of C1s (a), N1s (b) and Co2p (c) of the fresh, reused and regenerated CoNC_{M4}.

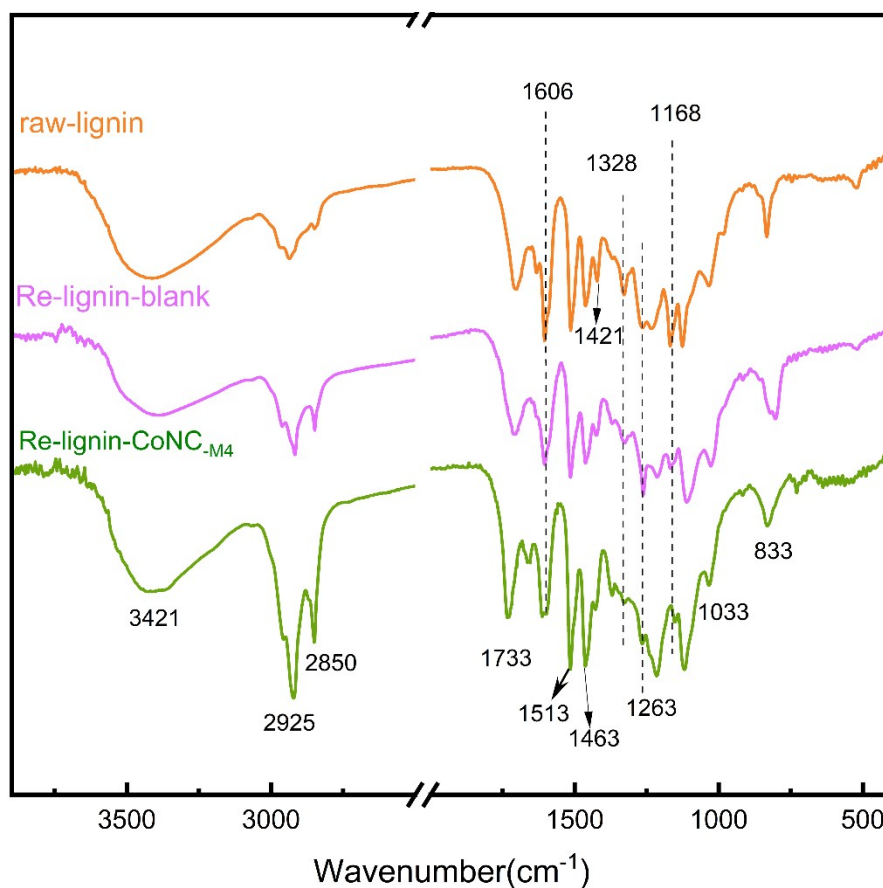
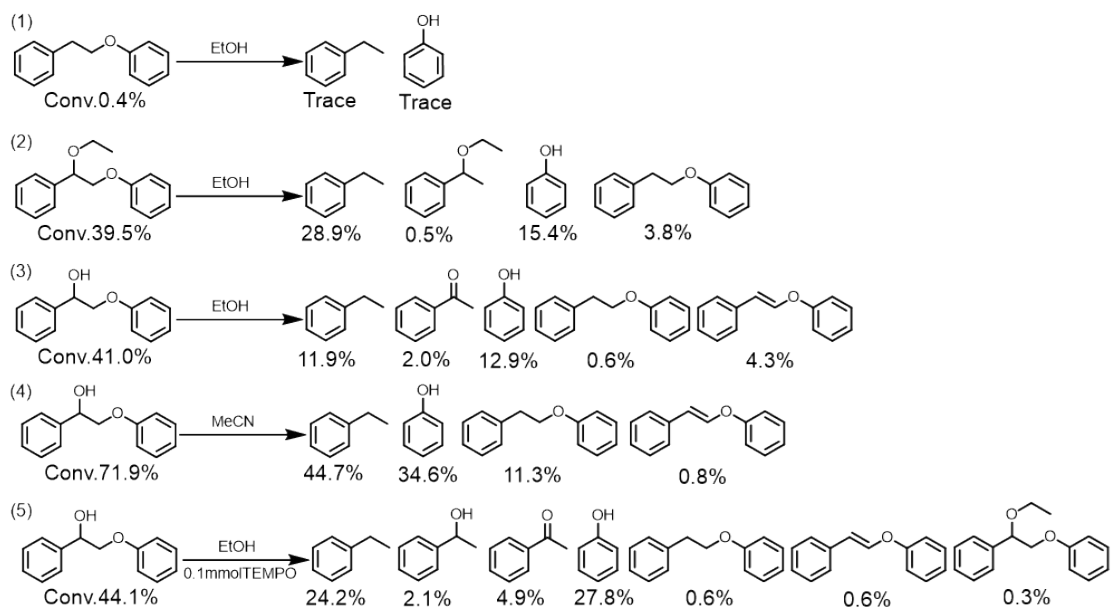
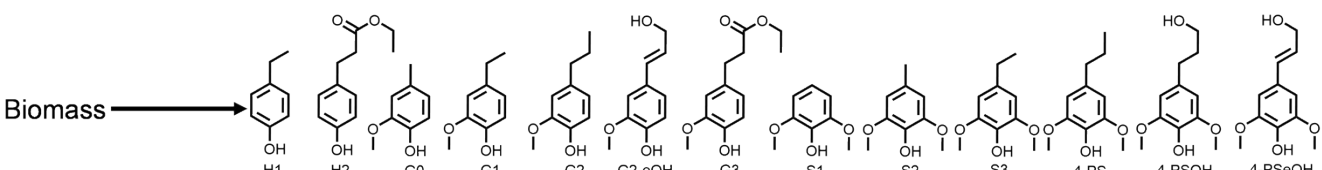


Fig. S11 FT-IR spectra of the raw-lignin, Re-lignin-blank and Re-lignin-CoNC_{M4}.



Scheme S1 Control experiments used to determine the reaction pathway. Conditions: substrate (0.2 mmol), catalyst (20 mg), solvents (10 mL), H₂ (1.0 MPa), 230°C, 4 h. (3) After stirring in a 1 mol L⁻¹ KOH solution for 5 h, the catalyst is filtered to obtain a solid, which is then washed three times with deionized water to obtain the catalyst.

Table S1 Comparison of reductive catalytic fractionation results over different catalysts in literatures.

							
Catalyst	Reaction conditions	Primary monomers	Yield/ wt. %		TON		Ref.
			4-PS	Monomers	4-PS	Monomers	
CoNC _{M4} (Co, 0.46 wt.%)	Organsolv bagasse lignin (0.1g), Catalyst (0.1g), 230°C, 1MPa H ₂ , 4h	4-PS	9.9	28.8	6.48	21.30	This work
Co ₁ Ti _{0.5} @BC (Co:4.5 wt.%)	0.5 g Enzymatic lignin (0.5g), 0.2 g Catalyst (0.2g), 250°C, 2MPa H ₂ , 4h.	H1, G1, G2	/	23.7	/	5.18	8
Co-Zn/Off-Al H-beta (Co: 1.24 wt.%)	Kraft lignin (0.5g), Catalyst (0.25g), 300°C, 2MPa H ₂ , 6h.	G0, G1	/	15.6	/	9.99	9
30Ni-Mg ₃ Al-LDOs (29.90 wt.%)	Organsolv bagasse lignin (0.2g), Catalyst (0.15g), 260°C, 1MPa Ar, 3h.	H1, G1	2.8	21.3	0.04	0.40	10
Ni ₅ Fe ₃ /Al ₂ O ₃ (Ni: 3.65 wt.%, Fe: 4.05 wt.%)	Beech sawdust (1g), Catalyst (0.2g), 250°C, 3MPa H ₂ , 3h	G2, 4-PS	12.2	27.2	2.32	5.37	11
Ni/C _f (14.77 wt.%)	Birch sawdust (0.1g), Catalyst (0.1g), 220°C, 2MPa H ₂ , 3h.	4-PS, 4-PSOH	19.3	45.2	0.39	0.94	12
CuO/C (Cu 82.40 wt.%)	Poplar sawdust (0.05g), Catalyst (0.025g), 240°C, 3MPa H ₂ , 4h.	4-PS, 4-PSOH	11.3	46.7	0.09	0.37	13
PtRe/TiO ₂ (Pt 2.00 wt.%)	Acid extracted birch lignin (0.2g), Catalyst (0.1g), 240°C, 1.5MPa He, 12h.	4-PS	7.5	18.7	7.44	19.95	14
Ru/C (5.00 wt.%)	Birch wood (150g), Catalyst (15g), 235°C, 3MPa H ₂ , 3h.	4-PS, G2	33.85	50.5	6.8	10.00	15
Pd/C (1.00 wt.%)	Birch wood (1g), Catalyst (0.25g), 200°C, 4MPa H ₂ , 15h.	G2, 4-PSOH	2.42	48.4	1.03	6.00	16
Mo ₁ Al/MgO (1.20 wt.%)	Eucalyptus wood (0.3g), Catalyst (0.1g), 200°C, 1MPa N ₂ , 8h.	G2-eOH 4-PSeOH	trace	46%	/	22.00	17

TON denotes turnover numbers, calculated based on the total number of moles of active metal in the catalyst ($\text{mol}_{\text{phenols}} \text{mol}_{\text{Active metal}}^{-1}$)

Table S2 Pore structure of catalysts.

Catalyst	Surface area (m ² g ⁻¹) ^a			Pore volume (cm ³ g ⁻¹) ^b			Mesoporous ratio (%) ^c
	S _{BET}	S _{micro}	S _{ext}	V _{total}	V _{micro}	V _{meso}	
CoNC _{M1}	380	248	132	0.27	0.13	0.14	51.9
CoNC _{M2}	646	159	487	0.40	0.09	0.31	77.5
CoNC _{M3}	1044	242	803	0.66	0.14	0.52	78.8
CoNC _{M4}	1394	137	1257	0.99	0.07	0.92	92.9
5 th CoNC _{M4}	52	6	46	0.11	0.003	0.107	97.3
CoNC _{M4}	1067	120	947	0.86	0.06	0.80	93.0
Regenerate							
CoC _{M4}	1709	37	1672	1.47	0.01	1.46	99.3
Co/NC _{M4}	1012	168	843	0.86	0.09	0.77	89.5
Co/AC	555	179	376	0.55	0.1	0.45	81.8
Ru/C	925	501	424	0.67	0.27	0.4	59.7
Pd/C	721	359	362	0.59	0.19	0.40	67.8

^a The surface area is determined utilizing the BET method. ^b The pore volume is evaluated through the BJH method. ^c The mesoporous ratio pore volume is calculated through $V_{\text{meso}}/V_{\text{Total}}$.

Table S3 Element analysis of the CoNC catalysts ^a.

Catalyst	Elemental content (wt.%)								
	N	C	H	S	O	Co	K	Na	Zn
CoNC _{M1}	6.90	71.64	2.08	0.27	18.08	1.03	0.11	0.06	0.06
CoNC _{M2}	3.10	59.41	3.07	1.84	30.78	1.80	0.20	0.15	0.03
CoNC _{M3}	5.10	56.42	3.06	0.37	24.17	10.88	0.14	0.09	1.37
CoNC _{M4}	8.61	70.76	2.38	1.95	15.84	0.46	0.12	0.10	0.03
NC _{M4}	/	/	/	/	/	/	0.11	0.06	1.19
CoC _{M4}	0.22	82.04	2.57	2.53	11.20	1.44	/	/	/
Co/NC _{M4}	4.73	68.96	2.82	0.43	25.56	0.50	/	/	/
CoNC _{M4} ^b	9.51	73.30	3.00	0.32	13.52	0.35	/	/	/

^a The Co, K, Na and Zn contents are detected by inductively coupled plasma atomic emission spectroscopy (ICP-OES), C, H, N, S contents are detected by elemental analysis. O content is calculated from the other element content. ^b CoNC_{M4} is obtained after five times reuse.

Table S4 N atomic relative content ratio and acidity of CoNC.

Catalyst	Relative amount (%)					Pyrrolic/ Pyridinic	Acidity ($\mu\text{mol g}^{-1}$)		Weak/ Total (%)
	Pyridinic- N	Co-N	Pyrrolic- N	Graphitic -N	Oxidized- N		Weak	Total	
CoNC _{M1}	34.01	15.66	22.23	19.76	8.34	0.65	162.98	376.10	43.33
CoNC _{M2}	26.29	16.53	22.01	28.78	6.39	0.84	307.31	465.90	65.96
CoNC _{M4}	32.69	12.02	21.21	23.21	10.87	0.65	111.71	273.29	40.88
NC _{M4}	33.33	/	31.41	24.04	11.22	0.94	200.08	658.61	30.38
NC _{M4-KOH}	40.94	/	16.56	28.85	13.65	0.40	/	/	/

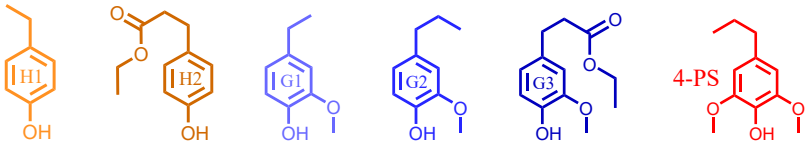
The amounts of acidic sites were determined according to the temperature and the area of the NH₃ desorption peaks.

Table S5 EXAFS fitting parameters at the Co K-edge various samples ($S_0^2=0.71$).

samples	path	C. N. ^[a]	R (Å) ^[b]	$\sigma^2 (\times 10^{-3} \text{ Å}^2)$ ^[c]	ΔE (eV) ^[d]	R factor ^[e]
Co foil	Co-Co	12*	2.51*	6.2	5.2	0.009
Co-sample	Co-N	4.3	2.08	6.5	2.0	0.012
	Co-Co	0.6	2.56	7.9		

^aC. N.: coordination numbers; ^bR: bond distance; ^c σ^2 : Debye-Waller factors; ^d ΔE_0 : the inner potential correction. ^eR factor: goodness of fit. *The experimental EXAFS fit by fixing C. N. as the known crystallographic value.

Table S6 Catalytic of various lignin samples over CoNC_{M4} catalyst^a.

							
Lignin		Yield wt.% ^b					
		H	G	4-PS	Others	Sel. _{4-PS}	Total
Hardwood	Birch	/	5.6	8.0	6.0	40.8	19.6
	Poplar	/	7.1	7.4	2.8	42.8	17.3
Softwood	Pine	/	11.1	0.6	3.3	4.0	15.0
	Chinese Fir	/	7.6	1.4	1.2	13.7	10.2
	Wheat bran	0.6	5.6	3.4	2.0	29.3	11.6
Grasses	Bamboo	2.5	5.2	7.2	4.1	37.9	19.0
	Corn cob	9.5	6.0	4.8	1.5	22.1	21.7

^a Conditions: organosolv lignin (100 mg), catalyst (100 mg), EtOH (10 mL), H₂ (1.0 MPa), 230°C, 4 h. ^b Yields were determined by GC-FID.

References

1. S. Liu, A. P. van Muyden, L. Bai, X. Cui, Z. Fei, X. Li, X. Hu and P. J. Dyson, *ChemSusChem*, 2019, **12**, 3271-3277.
2. Z. Li, Z. Cai, Q. Zeng, T. Zhang, L. J. France, C. Song, Y. Zhang, H. He, L. Jiang, J. Long and X. Li, *Green Chem.*, 2018, **20**, 3743-3752.
3. L. Li, J. Kong, H. Zhang, S. Liu, Q. Zeng, Y. Zhang, H. Ma, H. He, J. Long and X. Li, *Appl. Catal. B-Environ.*, 2020, **279**, 119343.
4. Y. Wang and S. Liu, *J. Agric. Food. Chem.*, 2024, **72**, 13320-13327.
5. A. Bahadoor, A. Brinkmann and J. E. Melanson, *Anal. Chem.*, 2021, **93**, 851-858.
6. M. Dolg, U. Wedig, H. Stoll and H. Preuss, *J. Chem. Phys.*, 1987, **86**, 866-872.
7. J. P. Perdew, K. Burke and M. Ernzerhof, *Phys. Rev. Lett.*, 1997, **78**, 1396-1396.
8. B. Luo, Z. Tian, R. Shu, C. Wang, Y. Chen, J. Liu and Y. Liao, *J. Catal.*, 2025, **442**.
9. X. Dou, X. Jiang, W. Li, C. Zhu, Q. Liu, Q. Lu, X. Zheng, H.-m. Chang and H. Jameel, *Appl. Catal. B-Environ.*, 2020, **268**, 118429.
10. Y. Tian, M. Gao, Z. Tang, F. Li, Q. Zeng, J. Long and X. Li, *J. Catal.*, 2024, **440**, 115833.
11. Z. Shen, W. Wang, L. Pan, Z. Huang, X. Zhang, C. Shi and J.-J. Zou, *Green Chem.*, 2023, **25**, 7782-7793.
12. K. Wu, B. Luo, K. Yang, S. Wang, M. Li and H. Zhang, *ACS Sustainable Chem. Eng.*, 2024, **12**, 1536-1547.
13. Q. Wang, L.-P. Xiao, Y.-H. Lv, W.-Z. Yin, C.-J. Hou and R.-C. Sun, *ACS Catal.*, 2022, **12**, 11899-11909.
14. J. Hu, S. Zhang, R. Xiao, X. Jiang, Y. Wang, Y. Sun and P. Lu, *Bioresour. Technol.*, 2019, **279**, 228-233.
15. Y. Liao, S.-F. Koelewijn, G. Van den Bossche, J. Van Aelst, S. Van den Bosch, T. Renders, K. Navare, T. Nicolai, K. Van Aelst, M. Maesen, H. Matsushima, J. M. Thevelein, K. Van Acker, B. Lagrain, D. Verboekend and B. F. Sels, *Science*, 2020, **367**, 1385-1390.
16. W. Lan, M. T. Amiri, C. M. Hunston and J. S. Luterbacher, *Angew. Chem. Int. Ed.*, 2018, **57**, 1356-1360.
17. G. Meng, W. Lan, L. Zhang, S. Wang, T. Zhang, S. Zhang, M. Xu, Y. Wang, J. Zhang, F. Yue, Y. Wu and D. Wang, *J. Am. Chem. Soc.*, 2023, **145**, 12884-12893.